

On the critical parameters for feasibility and advantage of air-breathing electric propulsion systems

Vittorio Giannetti^{a,b,*}, Eugenio Ferrato^{a,b}, Tommaso Andreussi^a

^a Institute of Mechanical Intelligence, Scuola Superiore Sant'Anna, Via Alamanni 13b, Pisa, 56010, Italy

^b Celeste S.r.l., Via Umberto Forti 6, Pisa, 56121, Italy

ARTICLE INFO

Keywords:

Air-breathing electric propulsion
Very low earth orbit
Drag compensation

ABSTRACT

In recent years, air-breathing electric propulsion emerged as a potential enabling technology for long-duration space missions in Very Low Earth Orbit (VLEO). In this work, we show how the complex relation between mission environment, spacecraft configuration, and propulsive performance can be associated to a single requirement for full air-breathing drag compensation, which becomes less stringent for higher VLEO orbits. The impact of the spacecraft shape and size on the performed analysis is then evaluated and the results compared with conventional electric propulsion solutions with stored propellant, showing how the adoption of air-breathing propulsion becomes more advantageous, from a volume and mass fraction perspective, when the spacecraft scale is reduced.

1. Introduction

The operation of space assets in Very Low Earth Orbit (VLEO), i.e., below an altitude of 400 km, would offer notable benefits over higher altitude missions [1,2]. First, operating closer to Earth's surface yields advantages for communication missions by reducing latency and transmission power while maintaining data link performance. It also improves Earth observation missions by enhancing reconnaissance conditions [3]. Lowering the spacecraft altitude allows for improved payload performance [4,5], enabling a potential reduction in the size of satellite platforms. Additionally, by operating below 250 km and within the high atmosphere, the spacecraft experiences lower radiation levels [6]. Moreover, VLEO offers the advantage of automatic re-entry and disposal due to atmospheric drag, which is an important feature considering the growing debris population [7].

However, to operate a satellite system in VLEO the significant drag experienced requires a propulsion system for compensation. This ties the platform's lifespan to the amount of propellant stored onboard and poses challenging requirements on the system design since the platform size and drag are influenced by the propellant mass. Therefore, apart from exceptional cases like GOCE [8,9] and SLATS [10], satellites typically do not operate in VLEO. SLATS was released at an altitude of 630 km and used a combination of chemical propulsion and aerobraking to lower its altitude to the 270–170 km altitude range, where an ion engine was used for drag compensation. In this VLEO phase of the mission, SLATS exhausted its 10 kg stored xenon propellant in 90 days. GOCE was released at an altitude of 283 km, it operated stably at

260 km for 2 years and 10 months and then its altitude was gradually lowered to 229 km, using xenon ion engines for drag compensation. GOCE stored 41 kg of propellant. It is worth noting that both spacecraft consumed the on-board stored propellant in just a few months when their altitude was lowered below 250 km.

The concept of an air-breathing electric rocket (AER) or air-breathing electric propulsion (ABEP) relies on an intake situated in front of the spacecraft to gather the same atmospheric particles that generate the drag. Utilizing electric power derived from solar arrays or batteries, an electric thruster then ionizes and accelerates these particles to generate thrust. By leveraging these limited yet renewable resources, it becomes possible to decouple the spacecraft's lifetime from the availability of propellant, enabling extended mission durations at low altitudes.

However, implementing the ABEP concept requires intricate system level trade-offs. For air-breathing systems, propulsive performance is closely intertwined with platform design and mission considerations. At a given altitude, the efficiency of energy transfer to atmospheric particles determines the feasibility of ABEP operation [11]. Below a certain altitude, the power required to accelerate the large collected flow exceeds the platform's capabilities, while above a different altitude, the ionization of the highly rarefied atmospheric flow becomes insufficient, making it impossible to deliver adequate power to the particles [12,13].

Based on available atmospheric models and flight data, several researchers have explored the characteristics of satellite platforms intended for VLEO operation and the feasibility of air-breathing electric

* Corresponding author at: Institute of Mechanical Intelligence, Scuola Superiore Sant'Anna, Via Alamanni 13b, Pisa, 56010, Italy.

E-mail address: vittorio.giannetti@santannapisa.it (V. Giannetti).

propulsion systems at altitudes below 300 km. An in depth review of the efforts in this direction can be found in Ref. [14]. The investigated concepts primarily focus on operations in sun-synchronous orbits at altitudes below 250 km, with a lifespan of several years, a spacecraft mass ranging from 100 kg to 1000 kg, and available power from solar arrays in the range of 0.3 kW to 3 kW [13,15–25].

Several propulsive technologies are being investigated for use on air-breathing systems, including Hall thrusters, Inductive Plasma Thrusters, Helicon thrusters, Gridded Ion Engines and others. The author is referred to Ref. [14] for a complete overview of the research efforts on these devices for ABEP applications. Many studies on air-breathing propulsion focused on a platform configuration based on a specific technological solution for the ABEP thruster. This is the case, for example, of the works of Hruby et al. [17,26], which investigated a Hall thruster based ABEP system for Earth and Mars operation. Similarly, Nishiyama [15] and Fujita [27] investigated the mission and system aspects related with the adoption of an air-breathing ECR ion engine as the ABEP system, considering a frontal area of 1.5 m² and an intake area of 0.48 m². A more general analysis was performed by Crisp et al. in Ref. [2], where the optimal VLEO altitude for optical and SAR-based missions was investigated, as well as a preliminary sizing of the main platform subsystems. They observed a circular dependence between the platform variables: as the orbit is lowered, more power is required to compensate the drag, but the larger solar surface area induces additional drag, further increasing the power requirement. This circular dependence forces some minimum performance requirements and, more generally, limits the region of convergence of the platform design. A similar result was found by Tisaev et al. [13], which obtained a narrow range of altitudes for the feasibility of the system, strongly dependent on the available specific impulse and thrust-to-power ratio of the air-breathing thruster. Finally, some recent works, including [13], have performed analyses on the orbit dynamics and feasibility of air-breathing systems, also including elliptical orbits [28], small scale spacecraft [25], and integrated optimization approaches [29].

In this work, we investigate air-breathing spaceflight from a general perspective, agnostic to the platform shape, scale, and propulsive technology. By doing so, the complex relation between mission environment, spacecraft configuration, and propulsive performance can be synthesized in a single, generally applicable, requirement for the feasibility of full ABEP drag compensation. Through this analysis, we define a global air-breathing system efficiency (η_{AER}), combination of the efficiency of all critical ABEP platform elements, and study how the minimum value for full drag compensation varies as a function of orbit and platform shape and size. A core merit parameter for the platform is then derived and some specific cases are investigated in greater detail: (i) a GOCE-like spacecraft (medium–large scale); (ii) a SLATS-like spacecraft (small scale) and (iii) a high-power 6U cubesat. When not available in the literature, the aerodynamic coefficients of the platform were derived through dedicated rarefied flow simulations employing a panel method, as described in Appendix.

In the second part of this study (Section 3), the previous conclusions are expanded in a systematic investigation of the core parameters determining the advantage of air-breathing systems over more traditional electric propulsion solutions with stored propellants from a mass and volume fraction perspective. Particularly, a scaling approach for the platform size is introduced and a first order method to evaluate the advantage of ABEP systems as a function of platform size and orbit altitude is proposed.

Ultimately, the proposed analysis provides a framework for the preliminary assessment of the feasibility of full air-breathing electric systems, identifying the core parameters and main trends for the minimum system requirements for full drag-compensation and to evaluate the advantage of ABEP over traditional systems as a function of orbit, platform scale and shape.

2. The air-breathing electric rocket efficiency

In an air-breathing system the intake is tasked with the efficient collection of the incoming atmospheric flow. Additionally, the intake shall compress the atmospheric flow to pressure conditions suitable for the efficient operation of the downstream electric thruster. The electric thruster then receives the atmospheric propellant collected and compressed by the intake, and ionizes and accelerates it to high speeds, generating an exhaust momentum flux and, thus, thrust (T). To enable sustained VLEO flight, the produced thrust should be equal or higher than the drag (D) generated by the incoming flow impinging on the system at orbital speed.

To investigate the conditions for feasibility of ABEP powered spaceflight we consider a generic spacecraft flying in VLEO with nominal attitude, aligned with the incoming atmospheric flow, having a total front surface A_t that intercepts a total atmospheric mass flow rate \dot{m}_i . We now assume that the spacecraft features a frontal intake of area A_i , intercepting an atmospheric mass flow rate \dot{m}_i , and that a mass flow rate \dot{m}_a reaches the electric thruster, as depicted in Fig. 1.

It is therefore possible to define several efficiencies for the system: the first one, denominated area efficiency η_A indicates how efficiently we are using the total (drag-inducing) frontal area to collect propellant.

$$\eta_A = \frac{A_i}{A_t} = \frac{\dot{m}_i}{\dot{m}_t}. \quad (1)$$

The second one, the collection efficiency, is a performance parameter of the intake and thruster chain, indicating what fraction of the mass flow rate impinging on the intake is transmitted to and processed by the subsequent electric thruster,

$$\eta_c = \frac{\dot{m}_a}{\dot{m}_i}. \quad (2)$$

A third crucial efficiency for the air-breathing system is the thrust efficiency of the electric thruster, which follows the conventional expression of Eq. (3) and represents how effectively the supplied power is used to generate thrust:

$$\eta_T = \frac{T^2}{2\dot{m}_a P}. \quad (3)$$

In Eq. (3) we have indicated with P the power supplied by the spacecraft for the operation of the electric thruster.

As already discussed, the condition for feasibility of ABEP powered spaceflight is that the thrust generated by the air-breathing system is sufficient to overcome the drag induced by the intercepted orbital flow,

$$T > D. \quad (4)$$

Given the definitions provided in previous paragraphs, with some simple algebra is possible to express the thrust as a function of the relevant efficiencies,

$$T = \sqrt{2\eta_A \eta_c \eta_T \dot{m}_i P}. \quad (5)$$

Observe that in these definitions, \dot{m}_i is the total mass flow rate intercepting the spacecraft frontal surface and thus is the same mass flow rate inducing drag on the spacecraft

$$\dot{m}_i = \rho_\infty u_\infty A_t, \quad (6)$$

where we have indicated with u_∞ and ρ_∞ respectively the asymptotic (orbital) velocity and mass density of the incoming flow.

Introducing the drag coefficient C_D , the drag can be conventionally expressed as

$$D = \frac{1}{2} C_D u_\infty^2 \dot{m}_i. \quad (7)$$

Therefore, the feasibility condition for ABEP flight becomes

$$\sqrt{2\eta_A \eta_c \eta_T \dot{m}_i P} > \frac{1}{2} C_D u_\infty^2 \dot{m}_i, \quad (8)$$

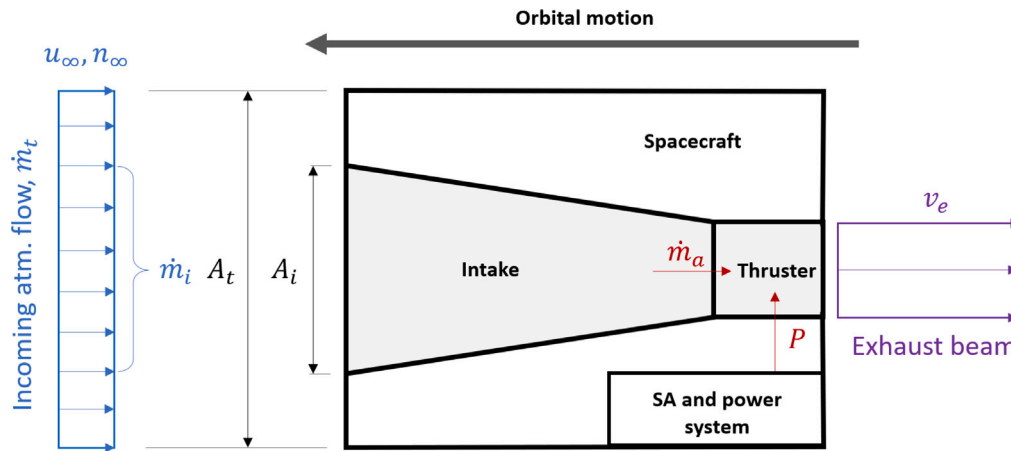


Fig. 1. Schematic of an ABEP propelled spacecraft.

that can be written as

$$\eta_A \eta_c \eta_T > \underbrace{\left[\frac{1}{2} \rho_\infty u_\infty^3 \right]}_O \bigg/ \underbrace{\left[\frac{4P}{C_D^2 A_t} \right]}_S \quad (9)$$

or equivalently

$$\eta_{AER} \doteq \frac{T^2}{2\dot{m}_i P} > \frac{O}{S}. \quad (10)$$

Here we have introduced a global air-breathing electric rocket efficiency $\eta_{AER} = \eta_A \eta_c \eta_T$, which corresponds to the product of the area, collection and thrust efficiency. Observe that the global ABEP efficiency retains a familiar form, analogous to the thrust efficiency but where the total asymptotic mass flow intercepted by the spacecraft is used instead of the propellant mass accepted into the thruster.

Upon more detailed investigation of the right hand side of Eq. (9), we identify that the minimum η_{AER} for mission feasibility corresponds to the ratio of two quantities: $O = \frac{1}{2} \rho_\infty u_\infty^3$ which is the asymptotic flux density of mechanical energy, and $S = \frac{4P}{C_D^2 A_t}$, which is a function of the

system design. The orbital parameter O is fundamentally a function of orbital altitude, although the atmospheric density is also affected by the local latitude/longitude coordinates, the day/night cycle, and the solar and geomagnetic activity. For what concerns the spacecraft parameter S , it is fundamentally a function of the platform shape, albeit the drag coefficient introduces a slight dependence on the asymptotic flow properties and composition. Interestingly, if one assumes a scaling approach that fixes P/A_t , the parameter S would be completely independent of scale. For example this is true when considering a scaling law that fixes the ratio between frontal and total lateral surface of the spacecraft (including the deployed solar arrays, if present) and assuming that the spacecraft dedicates a fixed fraction of the total available power to propulsion. In this case, at fixed platform configuration, the condition for ABEP flight feasibility would only be dependent on the target orbit (O), regardless of the spacecraft size.

Eq. (9) is equivalent to Eq. (4) and, thus, is a necessary and sufficient condition for feasibility of full air-breathing drag compensation. This implies that η_{AER} can be interpreted as a complete system efficiency and by monitoring only this performance parameter we can preliminary evaluate if a certain VLEO orbit (modulating O) will be accessible with air-breathing sustained flight for a certain platform design (S).

Some additional general conclusions can be drawn from Eq. (9):

- For a fixed orbit (O) and system (S) the feasibility requirement is imposed on the whole ABEP efficiency η_{AER} which is a product of multiple contributions. This implies that the requirement can be met by either increasing the collection efficiency of the intake, for

example by using highly specular materials [30], or by increasing the thruster efficiency, or by a combination of the two factors.

- The orbit parameter (O) rapidly decreases with altitude because of the sharp drop in atmospheric density. Fig. 2 reports the data extracted from the NRLMSISE-00 model [31] concerning the trend of the orbit-average atmospheric density, ρ_∞ , as a function of altitude (h), accounting for the 1σ variability associated with solar activity and location. This was computed by extracting the atmospheric data for the full 23rd solar cycle, from 1996 to 2008, with 30 days temporal resolution, 10 degrees latitude and 30 degrees longitude resolution, and by fitting a Gaussian distribution to find the global density average and variability. The rapid decrease of the orbit parameter implies that the overall ABEP efficiency requirement for sustained flight decreases for higher orbits and becomes, in principle, easier to achieve. Nevertheless, for higher orbits the atmospheric density will be lower and the electric thruster will need to operate with lower chamber pressures. The efficiency of electric thrusters is linked with propellant pressure [32] since the propellant ionization efficiency is strongly dependent on the local neutral particle density. This trend is apparent, for example, in [33] that reports the functional test results of a RIT-10 RF ion thruster operated with nitrogen and oxygen. The results show that, for a fixed thrust level, reducing the injected mass flow rate eventually leads to a sharp increase in the required RF power, and to the consequent drop of the total thrust efficiency, until the thruster becomes inoperable. This trend is true for all established electric thruster technologies, with some authors [13] even proposing a minimum neutral particle density required for operation at around 10^{18} m^{-3} . Therefore, even if the requirement on η_{AER} rapidly decreases with altitude, it is likely that a sufficiently high thrust efficiency η_T will be more difficult to achieve due to the reduction in atmospheric density.

- The merit parameter for the spacecraft characteristics for air-breathing spaceflight is

$$S = \frac{4}{C_D^2} \frac{P}{A_t}. \quad (11)$$

Which indicates how much power is dedicated to propulsion per unit frontal area, corrected by a factor accounting for the aerodynamic properties of the system. Aerodynamic, relatively small cross section spacecrafts which dedicate a significant portion of the total power to propulsion have a low C_D and a high P/A_t and will have a lower ABEP requirement for mission feasibility. This is somewhat intuitive as a high form factor, slender body will reduce the drag experienced by the spacecraft while maximizing the lateral surface area for propulsion power.

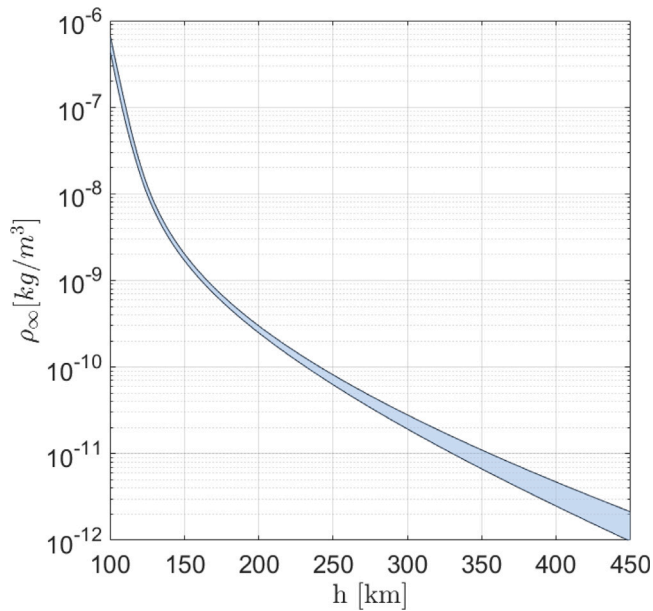


Fig. 2. Dependence of the atmospheric density as a function of altitude, h . The shaded area represent the 1σ variability with solar activity and location during the 23rd solar cycle. Values computed by means of the NRLMSISE00 atmospheric model [31,34].

The identified feasibility condition on η_{AER} can be expressed in different forms. For example a critical condition can be derived on the electric thruster specific impulse (I_{sp}), or equivalently on the effective exhaust velocity (v_e), by manipulating the same set of equations. Using the relationship between thrust and specific impulse $T = \dot{m}_a v_e = \dot{m}_a I_{sp} g_0$ one trivially obtains

$$v_e = g_0 I_{sp} > \frac{C_D}{2\eta_A \eta_c} u_\infty, \quad (12)$$

where g_0 is the standard gravity. If this condition is verified, the conditions of Eqs. (9) and (4) are automatically verified, and viceversa, as they are all equivalent feasibility criteria. The condition on I_{sp} does not provide information about the figures of merits of the platform shape as in Eq. (9), but it can provide a useful rule of thumb when evaluating the suitability of electric propulsion technologies for air-breathing systems. Indeed it tells us that the exhaust velocity of the electric propulsion device must be higher than the orbital velocity (u_∞) multiplied by a factor $\frac{C_D}{2\eta_A \eta_c}$, which primarily depends on the platform design and intake performance. Using realistic assumptions [14] on the drag coefficient ($C_D \approx 3 - 4$) and passive diffuse intake collection efficiency ($\eta_c \approx 0.2 - 0.5$) the minimum required specific impulse reaches values around 3000 s, similar to results obtained by other authors [13]. Even with highly optimistic assumptions, considering a $C_D = 2$ and $\eta_A \eta_c = 0.5$, the minimum effective exhaust velocity required for full drag compensation becomes $2u_\infty$. Considering an orbital velocity $u_\infty \approx 7800$ m/s the minimum required specific impulse would be $I_{sp,min} \approx 1590$ s. This already provides compelling evidence that high specific impulse technologies are required for feasible ABEP operation.

Eq. (9) can also provide some interesting insight on the power requirements for air-breathing drag compensation. After simple manipulation of the same equation, an equivalent condition can be derived on the minimum power that must be dedicated to propulsion (P)

$$P > \frac{C_D^2 \rho_\infty u_\infty^3 A_t}{8\eta_A \eta_c \eta_T}. \quad (13)$$

For a fixed orbit and spacecraft geometrical characteristics, Eq. (13) highlights how the required power for drag compensation is inversely proportional to the ABEP global efficiency. This was not immediately

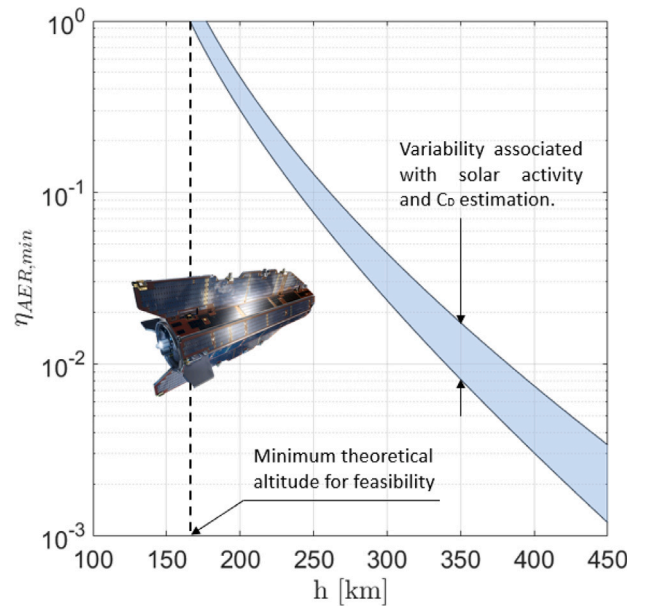


Fig. 3. Minimum air-breathing efficiency (in logarithmic scale) required for sustained air-breathing flight as a function of nominal orbital altitude for a GOCE-like spacecraft. The shaded area represents the uncertainties associated with the atmospheric density and composition and with the drag coefficient.

apparent from the condition on the minimum exhaust velocity Eq. (12) where, given a certain $\eta_A \eta_c$ it is always possible to identify a minimum specific impulse that ensures drag compensation. Eq. (13) specifically states that it is preferable to maximize the amount of mass flow collected by the ABEP system (maximizing $\eta_A \eta_c$) and to keep the specific impulse requirement as low as possible to minimize the power consumption for drag compensation.

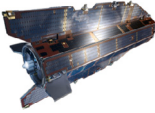
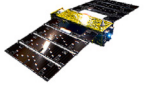
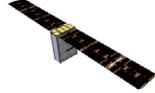
To consolidate and further expand the conclusions drawn from the feasibility condition of Eq. (9), we investigated the dependence of the minimum ABEP efficiency requirement for an hypothetical GOCE-like platform which maintains the core system features as the real GOCE spacecraft (such as size, external shape and available propulsion power), but that is propelled via an air-breathing system. To estimate the value of S for such a system, literature data available for the GOCE mission was used, employing a C_D between 3.6 and 4.1 [35], an A_t of 0.95 m², and a maximum power available for the propulsion system of 600 W [36]. For additional details see Appendix. With these assumptions, Fig. 3 reports the dependence of the minimum ABEP efficiency required for sustained air-breathing flight as a function of nominal orbital altitude for a GOCE-like spacecraft.

From this relatively simple analysis a number of interesting conclusions can be drawn. First of all, given a certain spacecraft design (S) there is an altitude limit below which an $\eta_{AER} > 1$ would be required for air-breathing drag compensation which is, by definition, impossible. For the investigated case, this minimum theoretical altitude limit is about 165 km. This implies that, regardless of the thruster and intake characteristics, below this altitude, ABEP flight becomes impossible for a circular orbit at constant altitude for this specific platform configuration. The minimum required η_{AER} then sharply drops with altitude, reaching values close to 0.1 around 250 km. As already mentioned, with increasing altitude, the requirement decreases rapidly because of the decrease in atmospheric density (and thus O) but, at the same time, the thruster has to achieve sufficient thrust efficiencies operating with a progressively lower pressure gas, which represents a technological challenge.

The values of Fig. 3 depend on the specific platform parameters adopted to calculate S . For example, only 600 W were used as propulsion power in the test case, which correspond to the maximum

Table 1

Investigated platform architectures and main parameters, including the newly defined platform merit parameter S . Credits for the GOCE image: ESA; Credits for the SLATS/Tsubame image: JAXA. Credits for the 6U CubeSat reference model: GomSpace.

Icon	Name	C_D [-]	A_f [m ²]	P [W]	S [W/m ²]
	GOCE-like	3.6–4.1	0.95	600	150–195
	SLATS-like	4.6–5.4	0.36	370	141–194
	High-power 6U CubeSat	5.8–7.1	0.03	60	159–238

propulsion power of the GOCE mission [36]. But, for different payloads, a larger fraction of the total 1600 W produced by the solar arrays could be used by the propulsion system. In this case the requirement on η_{AER} would be lower and the line of Fig. 3 would shift to lower altitudes.

To investigate the dependence of the minimum ABEP global requirement on the spacecraft parameters (S), a number of representative platform architectures were selected for evaluation, covering a wide range of possible spacecraft sizes and shapes. Specifically, we investigated a GOCE-like spacecraft, representative of medium/large VLEO satellites (≈ 1000 kg); a small-class SLATS-like spacecraft (≈ 300 kg), and a high-power 6U CubeSat (≈ 10 kg). Table 1 reports the main features of the selected architectures derived from the relevant literature, as described in Appendix. For what concerns the estimation of the C_D for the high-power 6U CubeSat, no information was available in the literature and, thus, a dedicated rarefied aerodynamic simulation based on the panel method was performed to estimate the drag coefficient (see Appendix).

It is interesting to note that, under certain circumstances, less aerodynamic shapes, like the 6U CubeSat, can have a higher merit parameter (S) than more aerodynamic systems, such as the GOCE-like spacecraft. This is mostly due to the fact that it dedicates a higher fraction of the total generated power to propulsion, increasing the ratio P/A_f . In general, the ratio of two crucial parameters determines the merit (S) of a certain spacecraft design: (i) P/A_f and (ii) C_D^2 . Both of these elements increase with the increase of the lateral solar arrays' area. The 6U CubeSat with very large solar arrays relative to its frontal surface, and which dedicates a significant fraction of the total power to propulsion, is capable of achieving high values of the merit parameter S even without an aerodynamic shape because the ratio P/A_f increased more than the corresponding increase in C_D^2 .

Fig. 4 depicts the trends of the minimum ABEP total efficiency, $\eta_{AER,min}$, requirement as a function of altitude, for the three spacecraft configurations of Table 1.

Even though large uncertainties are present due to the solar cycle and C_D estimation, Fig. 4 shows that a higher S parameter directly corresponds to a less stringent requirement on the minimum ABEP total efficiency for feasible ABEP sustained flight at a fixed altitude. It is worth noting that the scale of the spacecraft does not have a direct impact on the minimum ABEP total efficiency requirement but rather the ratio P/A_f does. Nevertheless, the capability of the system of complying with said requirement could depend on the system scale, since smaller propulsion systems typically achieve lower performance values compared with their larger scale counterpart.

Under the performed assumptions, these analyses clearly indicate the core parameters to be optimized in the early design of a platform system intended for VLEO ABEP flight and provide useful insight for a comparative assessment of possible spacecraft configurations.

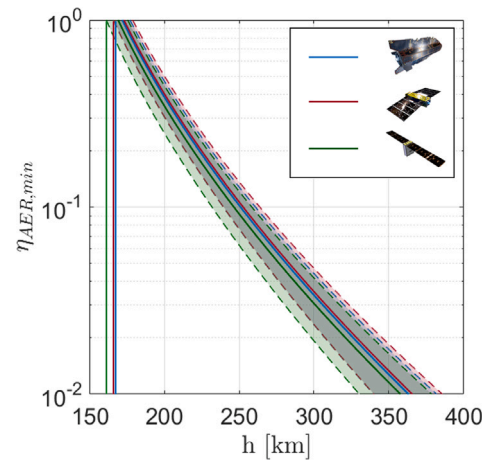


Fig. 4. Minimum ABEP efficiency required for sustained air-breathing flight as a function of nominal orbital altitude for different spacecraft shapes. The shaded area represents the uncertainties associated with the atmospheric density and composition and with the drag coefficient. Color-coded vertical lines indicate the theoretical minimum altitude for feasibility of the three spacecraft shapes. (For interpretation of the references to color in this figure legend, the reader is referred to the web version of this article.)

3. Comparison with stored propellant solutions

Consistently with what has been discussed in the previous section, if we can provide an ABEP system capable of satisfying the condition of Eq. (9) for the specific mission environment and platform under investigation, AER-based full drag compensation becomes feasible. Nevertheless, depending on the mission, the same task could also be performed with traditional electric propulsion systems using propellant stored onboard. It is, therefore, interesting to compare the effectiveness of ABEP systems and traditional electric propulsion systems in accomplishing the same mission at different platform scales, focusing on the locus of conditions for which air-breathing propulsion provides an advantage. Note that in the following we are only investigating the requirements for what concerns drag compensation, which becomes the most onerous task of the propulsion system at low altitudes.

Intuitively, since at first order the drag scales with the spacecraft frontal surface A_f , for a fixed mission duration performed with traditional EP systems also the total required onboard amount of propellant would scale with A_f . Smaller spacecraft would feature a lower total volume (V_f) and volume-to-surface ratio and, therefore, a comparatively smaller volume would be available to store the propellant.

Let us consider the ideal case of a spacecraft flying in VLEO for a nominal mission duration Δt , compensating the experienced drag (D) with a traditional electric propulsion system of constant thrust (T) with propellant stored onboard. Assuming $T = D$ we have that

$$I_{tot} = T \Delta t = D \Delta t = m_p v_e, \quad (14)$$

where we have defined I_{tot} and m_p as the total impulse and the total propellant mass required to perform the mission. Rearranging the terms and employing the expression for drag of Eq. (7) we arrive at an expression for the required propellant mass and volume (V_p)

$$m_p = \frac{D \Delta t}{v_e} = \frac{1}{2} C_D \rho_\infty u_\infty^2 A_f \frac{\Delta t}{v_e}, \quad (15)$$

$$V_p = \frac{m_p}{\rho_p} = \frac{1}{2} C_D \rho_\infty u_\infty^2 A_f \frac{\Delta t}{\rho_p v_e}, \quad (16)$$

where we have indicated with ρ_p the propellant storage density.

To investigate how the propellant mass and volume fraction scale with spacecraft size, we assume a uniform platform scaling law that preserves the spacecraft shape with a fixed aspect ratio α such that

the total platform volume $V_S = \alpha A_t^{3/2}$. Observe that with this scaling law, the ratio between frontal and lateral surface area is independent of scale. If one assumes that a fixed fraction of the total power generated via solar arrays is devoted to propulsion this also implies that the ratio P/A_t is preserved by the scaling. Therefore, with this rationale, the minimum ABEP efficiency requirement results to be independent of scale, but only depends on the selected orbit and platform shape. Ultimately one obtains for the propellant volume fraction the following expression:

$$\frac{V_p}{V_S} = \left[\frac{1}{2} \rho_\infty u_\infty^2 \right] \left[\frac{C_D}{\alpha \sqrt{A_t}} \right] \left[\frac{1}{\rho_p v_e} \right] \Delta t. \quad (17)$$

The mass fraction can be calculated considering that the total spacecraft wet mass, m_S , is the sum of the propellant mass, m_p , and of the mass of the non-propellant spacecraft elements $m_r = \rho_r (V_S - V_p)$

$$\frac{m_p}{m_S} = \frac{1}{1 + \frac{\rho_r}{\rho_p} \left(\frac{V_S}{V_p} - 1 \right)}, \quad (18)$$

where an average non-propellant spacecraft density parameter ρ_r was introduced.

Examining Eq. (17) some expected results are recovered:

- V_p/V_S and m_p/m_S are monotonically decreasing functions of altitude, since a lower thrust (and thus mass flow) is needed to compensate a lower drag;
- V_p/V_S and m_p/m_S are monotonically increasing functions of mission duration, since the drag needs to be compensated for a longer time;
- V_p/V_S is a monotonically decreasing function of propellant density (ρ_p) and thruster exhaust velocity (or equivalently specific impulse), since the propulsion system becomes more volume-efficient in storing the propellant and achieving the required total impulse with a lower amount of propellant. Note that the achievable specific impulse for a fixed thrust level is limited by the power available for propulsion.

For very high orbits, very little propellant is required for drag compensation, as the drag goes to zero. For very low orbits, instead, the mission becomes impractical as the drag is too high and a significant fraction of the total spacecraft volume would need to be dedicated to propellant storage. For certain conditions and mission durations, this becomes outright impossible ($\frac{V_p}{V_S}, \frac{m_p}{m_S} > 1$).

It is interesting to note that the propellant volume fraction is not scale-independent, but it is inversely proportional to the square root of the frontal area of the spacecraft. This implies that in smaller spacecraft, to complete the same mission with the same propellant and specific impulse, a larger volume fraction will be needed for propellant storage compared to a similar spacecraft of a larger size. A similar trend is also found for the mass fraction, albeit the density of the non-propellant elements of the spacecraft, ρ_r , could also change with platform size. Eq. (17) also highlights that the spacecraft shape parameter affecting the volume and mass ratios scaling with the characteristic length, $\sqrt{A_t}$, is C_D/α .

As an example analysis, Fig. 5 reports the dependence of the volume and mass fractions as a function of altitude for the compensation of the drag of a spacecraft with a GOCE-like shape via a traditional EP system with a specific impulse of 2000 s and a storage density of 1600 kg/m³, representative of a xenon electrostatic system [37], and a total mission duration of 5 years.

Adopting the scaling previously described, the mass and volume fractions are reported for two different platform scales. The blue lines report the behavior for an $A_t = 0.95 \text{ m}^2$, similar to the actual GOCE spacecraft, while the red lines are for $A_t = 0.95 \times 10^{-2} \text{ m}^2$, representative of the nanosat/CubeSat scale. To estimate the mass fraction when scaling down, two different cases are presented, considering an average

spacecraft density of the non-propellant elements of 200 kg/m³, similar to the real GOCE spacecraft, and of 1333 kg/m³, representative of typical CubeSat densities.

Note that in this sample analysis we have fixed the propulsive performance with scale. In reality, the thrusters' performance typically decrease at smaller scales. In general, it will be more complex to reach the same levels of specific impulse or thrust efficiency at small scale, thus requiring a relatively higher power to generate the required thrust.

As it is apparent from the figure, the platform scale has a significant impact on the propellant mass and volume fractions required to fulfill a drag compensation mission. Given the assumptions, if we consider, for example, a 250 km reference altitude, for the large platform the propellant would only require approximately 6% of the total spacecraft mass and less than 1% of the total volume. Note that the real GOCE spacecraft had a propellant mass fraction of about 4% at beginning of life (41 kg of propellant for a 1050 kg wet spacecraft mass) [8]. A direct comparison between the real GOCE mission (with its complex mission profile spanning several altitudes for different durations) and the reference GOCE-like fixed altitude 5 years drag compensation mission investigated here is, of course, not possible, but this confirms the right order of magnitude for the results of the analysis. To perform the same mission, the nano platform would need to dedicate from 10% up to 50% (depending on the spacecraft density) of the total mass and close to 10% of the total volume to propellant storage. This highlights how a drag compensation mission performed with stored propellant becomes comparatively more onerous, from a mass and volume perspective, at smaller spacecraft scales.

This is not the case for ABEP propulsion, where we can assume that a fixed fraction of the platform volume will be occupied by the intake of the air-breathing system, scaling with the spacecraft frontal surface and platform length. Under this assumption, given the volume fraction of the ABEP system, a breakeven platform size exists for every given altitude below which ABEP propulsion becomes advantageous from a volume perspective. Moreover, the lower the altitude the bigger the platform size breakeven point.

It is complex to define the volume fraction occupied by a generic ABEP system (V_{AER}/V_S) to compare with the propellant of a traditional EP system, since in ABEP configurations the intake would substitute not only the propellant itself but the complete propellant storage and management system. Therefore, we have performed a parametric study of the volume breakeven point against altitude and spacecraft size, considering an ABEP volume fraction ranging between 10% and 40% of the total spacecraft volume. Fig. 6 depicts the results of this analysis for the two extreme spacecraft configurations of GOCE-like and of our reference high-power 6U platform shape. Each line corresponds to the size-altitude combinations below which the ABEP system would occupy less volume than the propellant for our reference mission case. Note that in these plots only the average values for C_D and ρ_∞ were used to improve on the clarity of the presentation.

On the figure we have also reported the (scale-independent) minimum η_{AER} requirement for mission feasibility, as defined in Eq. (9). These results suggest that ABEP systems tend to become advantageous, from a volume fraction perspective, for lower altitudes and smaller spacecraft. Lowering the spacecraft size generally enlarges the range of altitudes for which ABEP propulsion becomes advantageous. Additionally, the advantage of ABEP systems at smaller scales for a larger range of orbits justifies the operation at higher altitudes in AER-mode, where the minimum ABEP system efficiency η_{AER} for mission feasibility is lower.

As it is apparent from the comparison between the left and right plots of Fig. 6 also the platform shape plays a crucial role in the determination of the breakeven lines for the volume occupancy of the ABEP and stored propellant cases. This study can thus be generalized as a function of the relevant platform shape parameter C_D/α (see Eq. (17)). The results are shown in Fig. 7 where we have selected a value of $V_{AER}/V_S = 0.3$ as a reference for the analysis. This two dimensional plot

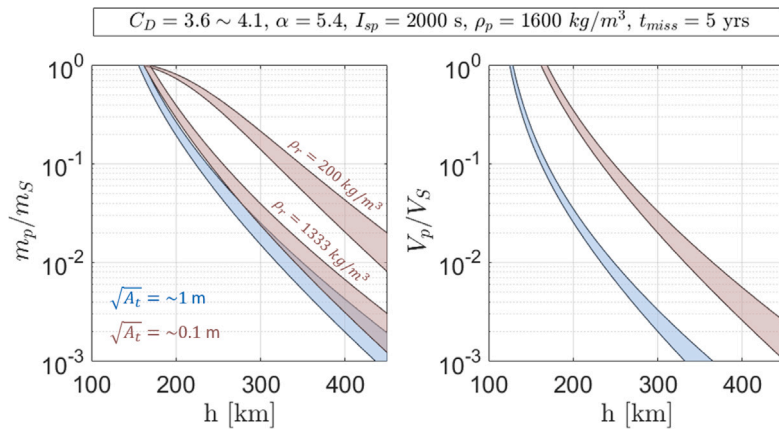


Fig. 5. Comparison of the mass and volume fractions occupied by a reference propellant for a 5 years drag compensation mission of a GOCE shaped platform of two different scales: $A_t = 0.95 \text{ m}^2$ in blue and $A_t = 0.95 \times 10^{-2} \text{ m}^2$ in red. (For interpretation of the references to color in this figure legend, the reader is referred to the web version of this article.)

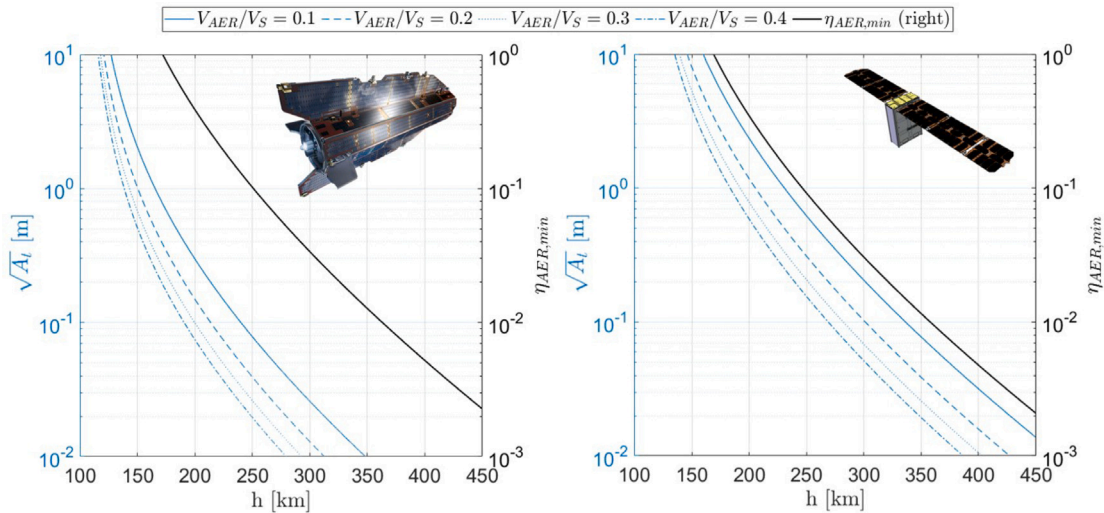


Fig. 6. Blue lines report ABEP vs. stored propellant volume fraction breakeven points for a 5 years drag compensation mission as a function of spacecraft size, altitude, and ABEP volume fraction for (left) a GOCE-like shape and (right) a reference high-power 6U CubeSat shape. black lines (right axis of the corresponding plot) report the minimum η_{AER} requirement for ABEP drag compensation mission feasibility (independent of scale). (For interpretation of the references to color in this figure legend, the reader is referred to the web version of this article.)

returns the characteristic length of the spacecraft ($\sqrt{A_t}$) below which the ABEP system would occupy less volume than the stored propellant solution for our reference drag compensation mission, as a function of altitude (h) and of the shape parameter of the spacecraft (C_D/α).

The results highlight once again how small scale spacecraft, regardless of the shape, extend the volume fraction advantage of ABEP over traditional EP systems to higher altitudes. Additionally, the figure shows how the advantage is more marked for less aerodynamic systems, with a higher C_D/α . This is expected as a more bluff body compensating the drag with a traditional EP system would require comparatively more propellant due to the higher C_D . It is in any case relevant since the platform shape could be driven by other considerations in addition to aerodynamics, such as payload allocation. Finally, the full comparison analysis was performed for an extended mission duration of 10 years (compared to the reference 5 years used in the previous discussion), to highlight the increasing advantage of air-breathing propulsion for longer drag compensation missions. Fig. 7 (right) reports the results for the break-even spacecraft size for the 10 years reference scenario,

showing how ABEP becomes more advantageous for a considerably larger range of altitudes when extending the duration of the mission.

Ultimately, these results are strongly dependent on the performed assumptions for the comparison, such as the propellant density, thruster specific impulse, mission duration and ABEP volume fraction, but the described analysis represents a useful approach to frame the feasibility of ABEP systems for specific mission cases and their competitiveness against traditional EP systems with stored propellants.

4. Conclusions

In this work we have presented a general investigation on the core parameters determining the feasibility and advantage of air-breathing electric propulsion systems for sustained drag compensation in very low Earth orbit. Starting from a general system-level analysis, the feasibility condition of producing a thrust (T) higher than the drag (D) was reformulated in terms of a minimum requirement on a newly defined air-breathing rocket efficiency, η_{AER} . This efficiency corresponds to

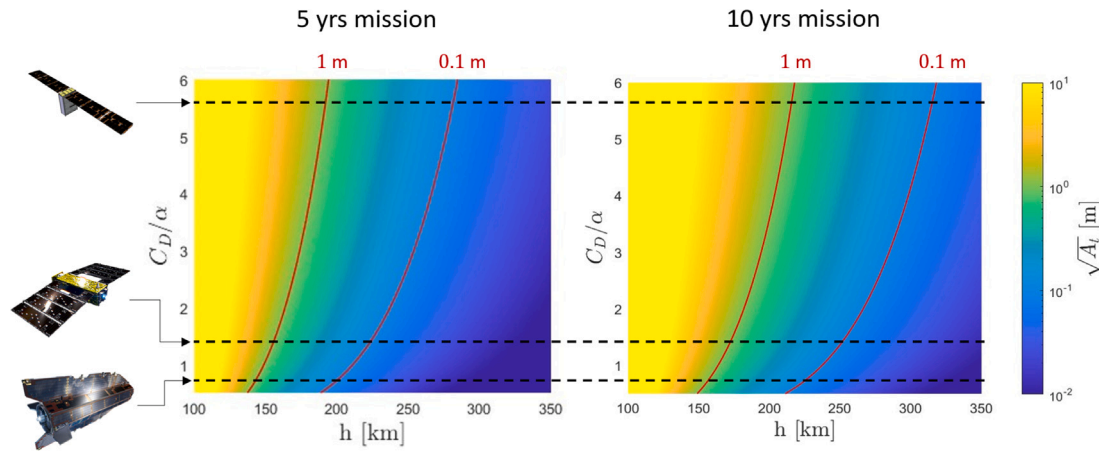


Fig. 7. Characteristic length of the spacecraft ($\sqrt{A_t}$) below which the ABEP system would occupy less volume than the stored propellant solution for a reference 5 years (left) and 10 years (right) drag compensation mission, as a function of altitude (h) and of the shape parameter of the spacecraft (C_D/α). A reference ABEP volume fraction of $V_{ABEP}/V_S = 0.3$ was assumed. Red lines highlight the 1 m and 0.1 m characteristic lengths. (For interpretation of the references to color in this figure legend, the reader is referred to the web version of this article.)

the product of three core parameters of the spacecraft and propulsion system design: the area efficiency, η_A , the intake collection efficiency, η_c , and the electric thruster thrust efficiency, η_T .

It was shown that the minimum requirement on η_{ABEP} for full drag compensation is equivalent to the ratio between two quantities, an orbital parameter O , that rapidly decreases with altitude, and a spacecraft parameter S , which is a function of the platform design. This novel formulation of the air-breathing drag compensation feasibility condition led to a number of non-trivial considerations. First of all, given a certain target orbit (O) and system design (S), the requirement is imposed on the global ABEP efficiency and, thus, it can be met by improving either the area, collection or thrust efficiency, or a combination of the three. Moreover, it was highlighted how a minimum altitude always exists, below which air-breathing drag compensation becomes physically impossible. We also showed how the minimum requirement on η_{ABEP} rapidly decreases with altitude because of the sharp decrease in atmospheric density. While this makes it easier to achieve in principle, the decrease in atmospheric density will also affect the capability of existing electric propulsion technologies of achieving sufficient ionization (and thus thrust) efficiencies.

The presented analysis led to the identification of the core spacecraft design merit parameter for air-breathing systems $S = \frac{4P}{C_D^2 A_t}$, which should be maximized to lower the minimum requirement on η_{ABEP} . To further highlight the dependence of the feasibility condition on the spacecraft design, a comparative analysis was performed by investigating three specific platforms of various sizes: (i) a GOCE-like spacecraft, (ii) a SLATS-like spacecraft, and (iii) a reference high-power 6U CubeSat. The results show that the scale of the spacecraft does not have a direct impact on the minimum ABEP total efficiency requirement but rather the ratio between the propulsive power and the frontal area does. It is nevertheless worth noting that, while the requirement does not directly depend on size, the capabilities of the propulsion system of achieving sufficient efficiency to meet the requirement will, as smaller propulsion are typically limited in the performance figures they can reach. Additionally, the derived requirement on η_{ABEP} is a local, instantaneous requirement for drag compensation along the VLEO orbit. For complex and perturbed mission profiles, if the requirement is verified for every point along the orbit the ABEP system always provides a net thrust, but more refined analysis could identify a less stringent orbit-average requirement for feasibility. Finally, it was noted that the parameter S benefits from a more aerodynamic shape (lowering C_D) but, in general, less aerodynamic shapes can still achieve a high merit

parameter by having a large lateral (power generating) surface area and by dedicating a larger fraction of the generated power to propulsion.

Building on these results, in the second part of this study, we presented a framework for the comparison, in terms of mass and volume fraction, between air-breathing systems and traditional electric propulsion with stored propellant using, as a reference, a xenon, $I_{sp} = 2000$ s technology. To investigate the dependence of the comparison on the platform scale, we introduced a uniform platform scaling law that preserves the spacecraft shape with a fixed aspect ratio, α . For a reference drag compensation mission of 5 years, we have highlighted how the propellant volume and mass fractions of traditional systems depend on the spacecraft scale ($\sqrt{A_t}$) because of the variability in the surface-to-volume ratio of the platform. Assuming, as a first approximation, that the intake of an ABEP system would occupy a fixed fraction of the platform volume, we have shown that a breakeven platform size exists for every given altitude below which ABEP propulsion becomes advantageous from a volume occupancy perspective. This breakeven platform size clearly depends on the selected mission duration, propulsion system characteristics, spacecraft shape, and reference altitude. In general, since the propellant allocation for drag compensation is more onerous for small platforms, ABEP systems show greater competitiveness for small spacecraft sizes across a wider range of altitudes, where the $\eta_{ABEP,min}$ is lower. Finally, to demonstrate the dependence of the results on the spacecraft shape, we have repeated the analysis as a function of the relevant platform shape parameter C_D/α . The results show how the advantage is more marked for less aerodynamic systems, since a more bluff body compensating the drag with traditional electric propulsion would require comparatively more propellant. This could be relevant for all cases where the platform shape could be driven by other considerations in addition to aerodynamics, such as payload allocation. Finally, the analysis was repeated for an extended mission duration of 10 years, quantitatively assessing the intuitive concept that ABEP becomes more attractive for a larger range of altitudes and spacecraft sizes when the duration of the mission is increased.

Concluding, this work has presented a framework for the investigation of the feasibility and advantage of air-breathing electric propulsion systems, proposing a single requirement in terms of the ABEP efficiency, and providing general guidelines on the core parameters to optimize in terms of propulsive performance, orbit selection, and platform shape and size.

CRediT authorship contribution statement

Vittorio Giannetti: Conceptualization, Data curation, Formal analysis, Investigation, Methodology, Software, Supervision, Validation, Visualization, Writing – original draft, Writing – review & editing. **Eugenio Ferrato:** Data curation, Formal analysis, Investigation, Methodology, Software, Visualization, Writing – original draft, Writing – review & editing. **Tommaso Andreussi:** Conceptualization, Funding acquisition, Project administration, Resources, Supervision, Writing – original draft, Writing – review & editing.

Declaration of competing interest

The authors declare that they have no known competing financial interests or personal relationships that could have appeared to influence the work reported in this paper.

Acknowledgments

The work performed at the Scuola Superiore Sant’Anna was supported by the European Research Council in the framework of the “Building a space Revolution: Electric Air-breathing Technology for High-atmosphere Exploration (BREATHE)” project, under HORIZON ERC-2022-COG grant number 101088694;

Appendix. Estimation of platform parameters

To appreciate the impact of the spacecraft scale and configuration on the analysis presented in this work, we have considered the three reference spacecraft listed in Table 1. They include the large/medium-class GOCE platform, the small-class SLATS platform, and a high-power 6U CubeSat platform.

In general, in free molecular flows the drag coefficient C_D is affected by several variables, such as flow properties, wall material, temperature, and geometry [38], and should be estimated from a detailed assessment of flow properties and platform geometry and thermal behavior. Moreover, in air-breathing platforms the flow interaction with the intake internal surfaces and the fact that a fraction of the incident particles are processed and expelled by the thruster add more uncertainty in the drag estimation. The detailed quantification of the impact of these processes on the resulting drag coefficient would involve complex DSMC and plasma simulations which are beyond the scope of this simplified analysis. In general, the intake drag (net momentum flux through A_i) will be the sum of the incident particle momentum flux at orbital velocity and the momentum flux of the particles effusing back at the velocity thermalized at wall temperature. As the wall thermalized velocity is more than an order of magnitude lower than the orbital velocity, the impact on the resulting drag of particles effusing back is in general small compared to the incident particle contribution. Considering that the number of particles effusing back is equal to the incident particles multiplied by the factor $1 - \eta_c$, being η_c the ABEP collection efficiency, the difference of drag between a closed frontal surface, i.e., $\eta_c = 0$, and the ABEP configuration is considered a second order correction.

Additionally, note that some authors identify different contributions to the drag coefficient for the frontal, lateral and solar panels drag, which must then be weighted to the corresponding surface to estimate the full drag (see for example Ref. [13]). In this work, we are only using the overall spacecraft drag coefficient C_D which accounts for the full drag, D , acting on the spacecraft (including all lateral surfaces) and uses as a reference surface the spacecraft frontal area A_f ,

$$C_D = \frac{2D}{\rho_\infty u_\infty^2 A_f}. \quad (\text{A.1})$$

Following the above considerations, the reference value range of drag coefficient for the GOCE platform was taken according to the

Table A.2

Drag coefficient of high-power 6U CubeSat platform in nominal attitude, computed by ADBSat for altitudes between 150 km and 300 km, energy accommodation coefficients between 0.9 and 1, and a wall temperature of 300 K. The Sentman GSI model has been employed.

	$h = 150$ km	200 km	250 km	300 km
$\alpha = 0.9$	6.46	6.83	7.03	7.15
0.95	6.22	6.60	6.79	6.92
1	5.78	6.17	6.37	6.50

work presented in [35], where a combination of numerical methods and flight data are used to estimate the drag experienced by GOCE during its lifetime. This results, depending on the model used, in a C_D between 3.7 and 4.1 for the reference platform frontal area of 0.95 m². Based on the data reported in [36], we consider 600 W of power available to its on-board propulsion system, corresponding to the maximum throttling capability of the GOCE ion thrusters and a thrust level of 20 mN.

Due to the lack of more recent aerodynamic data available in the literature, in this work we consider the rarefied flow simulation results reported in [10] for a preliminary but still representative design of the SLATS platform. By considering a value of 7.2 m² as a reference frontal area (corresponding to the platform solar array surface area), the work cited makes use of the Maxwell Gas–Surface Interaction (GSI) model to assess the aerodynamic force and momentum coefficients depending on the spacecraft angle of attack and sideslip angle. At nominal attitude, a longitudinal force coefficient between 0.23 and 0.27 is computed, translating into a C_D between 4.6 and 5.4 when the actual 0.36 m² of platform frontal area is considered. Consistently with the data reported in [39], we assume 370 W of power available to the propulsion subsystem, corresponding to a 10 mN thrust level produced by the ion thruster embarked in the SLATS platform.

Concerning the aerodynamic behavior of CubeSats, very few data seem available in the literature. As such, we made use of the recently developed ADBSat suite [40] to assess the aerodynamic behavior of a reference high-power 6U CubeSat. ADBSat is a software based on a novel implementation of a panel method which is capable of determining the aerodynamic properties of any body in free-molecular flow. In ADBSat, the body is represented as a set of fundamental elements and the sum of their individual aerodynamic properties makes up the properties of the whole. These are read from the meshing elements of an input CAD geometry file in the Wavefront format. In our analysis, we make use of the GOMspace 6U structure and NanoPower TSP deployable solar arrays CAD files, which are openly available in the GOMspace website [41]. According to the available datasheet, a 6U CubeSat equipped with two NanoPower TSP solar arrays is capable of producing up to 100 W of available power in fully illuminated condition, which is consistent with our choice of 60 W as a reference power level available to the propulsion subsystem. The platform 3D model was meshed in FreeCAD environment [42] and imported into the ADBSat toolbox. Fig. A.8 shows the imported meshed geometry along with the model output in terms of pressure coefficient distribution for a reference simulation case.

A reasonable range for the CubeSat platform drag coefficient variability was then assessed by performing twelve simulations for different combinations of altitudes and wall energy accommodation coefficients, see Table A.2. We considered reference altitudes of 150 km, 200 km, 250 km, and 300 km, while the wall accommodation coefficient was varied between 0.9 and 1, which is consistent with the estimations based on flight measurements reported in [43]. Consistently with the ADBSat validation approach presented in [44], we employed the Sentman GSI model, chose 19 January 2015 midnight 0°/0° latitude/longitude as reference time and geographic coordinates, and set the 81-day average F10.7 to 138.1, the daily F10.7 to 121.7, and the Ap magnetic indices in the 2.9 to 9.0 range. Accordingly, a C_D between 5.78 and 7.15 for a 0.03 m² frontal area was obtained from the simulations.

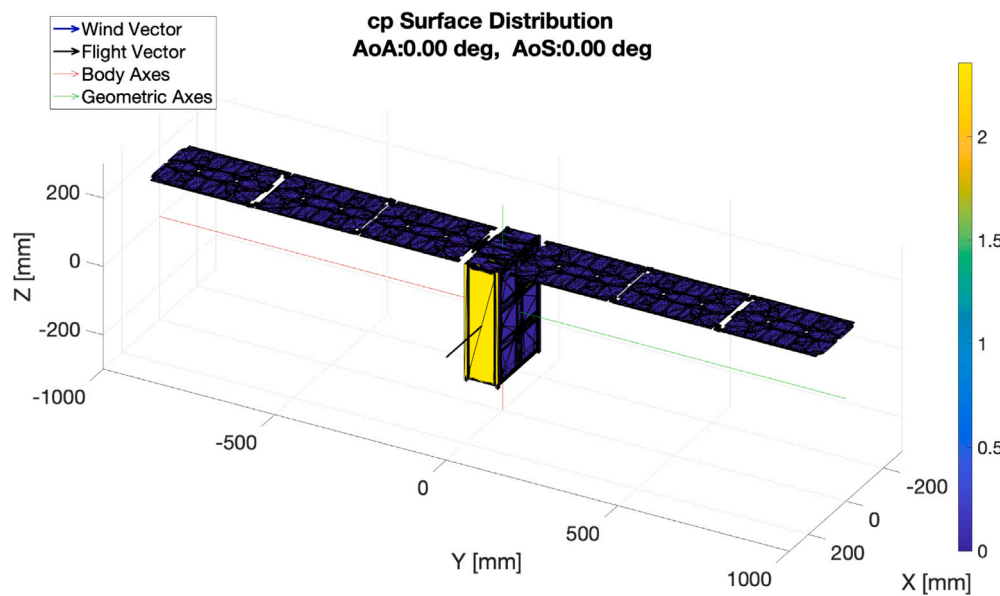


Fig. A.8. Example of ADBSat output in terms of pressure coefficient distribution for a simulated altitude of 250 km and an energy accommodation coefficient of 0.95.

References

- [1] N.H. Crisp, P.C. Roberts, S. Livadiotti, V.T. Oiko, S. Edmondson, S.J. Haigh, C. Huyton, L.A. Sinpetru, K.L. Smith, S.D. Worrall, J. Becedas, R.M. Domínguez, D. González, V. Hanessian, A. Mølgaard, J. Nielsen, M. Bisgaard, Y.A. Chan, S. Fasoulas, G.H. Herdrich, F. Romano, C. Traub, D. García-Almiñana, S. Rodríguez-Donaire, M. Sureda, D. Kataria, R. Outlaw, B. Belkouchi, A. Conte, J.S. Perez, R. Villain, B. Heißerer, A. Schwalber, The benefits of very low earth orbit for earth observation missions, *Prog. Aerosp. Sci.* 117 (September) (2020) <http://dx.doi.org/10.1016/j.paerosci.2020.100619>, [arXiv:2007.07699](https://arxiv.org/abs/2007.07699).
- [2] N.H. Crisp, P.C. Roberts, F. Romano, K.L. Smith, V.T. Oiko, V. Sullioti-Linner, V. Hanessian, G.H. Herdrich, D. García-Almiñana, D. Kataria, S. Seminari, System modelling of very low earth orbit satellites for earth observation, *Acta Astronaut.* 187 (June) (2021) 475–491, <http://dx.doi.org/10.1016/j.actaastro.2021.07.004>.
- [3] P. Kansakar, F. Hossain, A review of applications of satellite earth observation data for global societal benefit and stewardship of planet earth, *Space Policy* 36 (2016) 46–54, <http://dx.doi.org/10.1016/j.spacepol.2016.05.005>.
- [4] C. McGrath, C. Lowe, M. Macdonald, S. Hancock, Investigation of very low earth orbits (VLEOs) for global spaceborne lidar, *CEAS Space J.* (0123456789) (2022) <http://dx.doi.org/10.1007/s12567-022-00427-2>.
- [5] A. Moreira, P. Prats-Iraola, M. Younis, G. Krieger, I. Hajnsek, K.P. Papathanassiou, A tutorial on synthetic aperture radar, *IEEE Geosci. Remote Sens. Mag.* 1 (1) (2013) 6–43, <http://dx.doi.org/10.1109/MGRS.2013.2248301>.
- [6] L.M.S. Martines, Analysis of LEO Radiation Environment and its Effects on Spacecraft's Critical Electronic Devices (Ph.D. thesis), Embry-Riddle Aeronautical University, 2011, URL: <https://commons.erau.edu/edt/102>.
- [7] J.N. Peltou, S. Madry, S. Camacho-Lara, Handbook of satellite applications, in: *Handbook of Satellite Applications*, Vol. 1–2, 2013, pp. 1–1228, <http://dx.doi.org/10.1007/978-1-4419-7671-0>.
- [8] M.R. Drinkwater, R. Floberghagen, R. Haagmans, D. Muzi, A. Popescu, GOCE: ESA's first earth explorer core mission, in: *Proceedings of an ISSI Workshop 11–15 March 2002, Bern, Switzerland, 2003*, pp. 419–432, <http://dx.doi.org/10.1007/978-94-017-1333-736>.
- [9] C. Steiger, M. Romanazzo, P.P. Emanuelli, R. Floberghagen, M. Fehringer, The deorbiting of ESA's gravity mission GOCE - spacecraft operations in extreme drag conditions, in: *13th International Conference on Space Operations, SpaceOps 2014*, 2014, pp. 1–12, <http://dx.doi.org/10.2514/6.2014-1934>.
- [10] K. Fujita, A. Noda, Rarefied aerodynamics of a super low altitude test satellite, in: *41st AIAA Thermophysics Conference*, 2009, pp. 22–25, <http://dx.doi.org/10.2514/6.2009-3606>, June.
- [11] E. Ferrato, V. Giannetti, M. Tisaev, A. Lucca Fabris, F. Califano, T. Andreussi, Rarefied flow simulation of conical intake and plasma thruster for very low earth orbit spaceflight, *Front. Phys.* 10 (March) (2022) 1–17, <http://dx.doi.org/10.3389/fphy.2022.823098>.
- [12] T. Andreussi, E. Ferrato, C.A. Paissoni, A. Kitaeva, V. Giannetti, A. Piragino, A. Rossodivita, S. Schaeff, K. Katsonis, C. Berenguer, Z. Kovacova, E. Neubauer, M. Tisaev, B. Karadag, A.L. Fabris, M. Smirnova, A. Mingo, D. Le Quang, Z. Alsalihi, F. Bariselli, P. Parodi, P. Jorge, T.E. Magin, AETHER air breathing electric thruster: Towards very low earth orbit missions, in: *Proceedings of the 72nd International Astronautical Congress, IAC, IAC-21,C4,5,x66453*, 2021.
- [13] M. Tisaev, E. Ferrato, V. Giannetti, C. Paissoni, N. Baresi, A. Lucca Fabris, T. Andreussi, Air-breathing electric propulsion: Flight envelope identification and development of control for long-term orbital stability, *Acta Astronaut.* 191 (October 2021) (2022) 374–393, <http://dx.doi.org/10.1016/j.actaastro.2021.11.011>.
- [14] T. Andreussi, E. Ferrato, V. Giannetti, A review of air-breathing electric propulsion: from mission studies to technology verification, *J. Electr. Propuls.* 1 (1) (2022) 1–57, <http://dx.doi.org/10.1007/s44205-022-00024-9>.
- [15] K. Nishiyama, Air breathing ion engine concept, in: *54th International Astronautical Congress*, Vol. 3, 2003, pp. 383–390, <http://dx.doi.org/10.2514/6.iac-03-s.4.02>, October.
- [16] D. Di Cara, J. Gonzalez del Amo, A. Santovicenzo, B. Carnicero Dominguez, M. Arcioni, A. Caldwell, I. Roma, RAM electric propulsion for low earth orbit operation: an ESA study, in: *30th International Electric Propulsion Conference, Florence, Italy, IEPC-2007-162*, 2007.
- [17] V. Hruby, K. Hohman, J. Szabo, Air breathing hall effect thruster design studies and experiments, in: *37th International Electric Propulsion Conference, Boston, Massachusetts, IEPC-2022-446*, 2022.
- [18] K. Diamant, A 2-stage cylindrical hall thruster for air breathing electric propulsion, in: *46th AIAA/ASME/SAE/ASEE Joint Propulsion Conference*, 2010, <http://dx.doi.org/10.2514/6.2010-6522>.
- [19] A. Shabshelowitz, Study of RF Plasma Technology Applied to Air-Breathing Electric Propulsion (Ph.D. thesis), University of Michigan, 2013.
- [20] T. Schönherr, G. Han, C. Gürbüz, H. Koizumi, K. Komurasaki, First experiments towards an atmosphere-breathing PPT, in: *34th International Electric Propulsion Conference, Kobe, Japan, IEPC-2015-272*, 2015.
- [21] F. Romano, B. Massuti-Ballester, T. Binder, G. Herdrich, S. Fasoulas, T. Schönherr, System analysis and test-bed for an atmosphere-breathing electric propulsion system using an inductive plasma thruster, *Acta Astronaut.* 147 (March 2017) (2018) 114–126, <http://dx.doi.org/10.1016/j.actaastro.2018.03.031>, [arXiv:2103.02328](https://arxiv.org/abs/2103.02328).
- [22] T. Andreussi, E. Ferrato, V. Giannetti, A. Piragino, G. Cifali, M. Andreucci, C.A. Paissoni, Development status and way forward of SITAE's air-breathing electric propulsion engine, in: *AIAA Propulsion and Energy Forum and Exposition, 2019*, <http://dx.doi.org/10.2514/6.2019-3995>.
- [23] M.Y. Ovchinnikov, Y.V. Mashtakov, D.S. Roldugin, Mathematical modeling of the dynamics of a low-flying spacecraft with a ramjet electric propulsion engine, *Math. Models Comput. Simul.* 14 (2022) 452–465, <http://dx.doi.org/10.1134/S2070048222030139>.
- [24] S. Vaidya, C. Traub, F. Romano, S. Rodriguez-Donaire, D. Garcia-Almiñana, M. Sureda, M. Garcia-Berenguer, Development and analysis of novel mission scenarios based on atmosphere-breathing electric propulsion (ABEP), *CEAS Space J.* (2022) 1–18, <http://dx.doi.org/10.1007/s12567-022-00436-1>, URL: <https://link.springer.com/article/10.1007/s12567-022-00436-1>.
- [25] P. Crandall, R. Wirz, Air-breathing electric propulsion: mission characterization and design analysis, *J. Electr. Propuls.* 1 (12) (2022) 931–937, <http://dx.doi.org/10.1007/s44205-022-00009-8>.
- [26] V. Hruby, B. Pote, T. Brogan, K. Hohman, J. Szabo, P. Rostler, Air breathing electrically powered hall effect thruster, 2004, United States Patent US 6834492 B2.

- [27] K. Fujita, Air intake performance of air breathing ion engines, *J. Jpn. Soc. Aeronaut. Space Sci.* 52 (610) (2004) 514–521, <http://dx.doi.org/10.2322/jjsass.52.514>.
- [28] Y. Yue, J. Geng, G. Feng, W. Li, Elliptical orbit design based on air-breathing electric propulsion technology in very-low earth orbit space, *Aerospace* 10 (2023) <http://dx.doi.org/10.3390/aerospace10100899>.
- [29] A. Golikov, A. Filatyev, Integrated optimization of trajectories and layout parameters of spacecraft with air-breathing electric propulsion, *Acta Astronaut.* 193 (2022) 644–652, <http://dx.doi.org/10.1016/j.actaastro.2021.06.052>.
- [30] F. Romano, J. Espinosa-Orozco, M. Pfeiffer, G. Herdrich, N.H. Crisp, P.C. Roberts, B.E. Holmes, S. Edmondson, S. Haigh, S. Livadiotti, A. Macario-Rojas, V.T. Oiko, L.A. Sinpetru, K. Smith, J. Becedas, V. Sullioti-Linner, M. Bisgaard, S. Christensen, V. Hanessian, T.K. Jensen, J. Nielsen, Y.A. Chan, S. Fasoulas, C. Traub, D. García-Almiñana, S. Rodríguez-Donaire, M. Sureda, D. Kataria, B. Belkouchi, A. Conte, S. Seminari, R. Villain, Intake design for an atmosphere-breathing electric propulsion system (ABEP), *Acta Astronaut.* 187 (May) (2021) 225–235, <http://dx.doi.org/10.1016/j.actaastro.2021.06.033>, [arXiv:2106.15912](https://arxiv.org/abs/2106.15912).
- [31] J. Picone, A.E. Hedin, D.P. Drob, A.C. Aikin, NRLMSISE-00 empirical model of the atmosphere: Statistical comparisons and scientific issues, *J. Geophys. Res.* 107 (A12) (2002) 1468, <http://dx.doi.org/10.1029/2002JA009430>.
- [32] V. Giannetti, A. Piragino, C.A. Paissoni, E. Ferrato, D. Estublier, T. Andreussi, Experimental scaling laws for the discharge oscillations and performance of hall thrusters, *J. Appl. Phys.* 131 (2022) <http://dx.doi.org/10.1063/5.0070945>.
- [33] G. Cifali, T. Misuri, P. Rossetti, M. Andrenucci, D. Valentian, D. Feili, Preliminary characterization test of HET and RIT with nitrogen and oxygen, in: 47th AIAA/ASME/SAE/ASEE Joint Propulsion Conference and Exhibit 2011, American Institute of Aeronautics and Astronautics Inc., 2011, <http://dx.doi.org/10.2514/6.2011-6073>.
- [34] J. Picone, A. Hedin, D. Drob, R. Meier, J. Lean, A. Nicholas, S. Thonnard, Enhanced empirical models of the thermosphere, *Phys. Chem. Earth C* 25 (5) (2000) 537–542, [http://dx.doi.org/10.1016/S1464-1917\(00\)00072-6](http://dx.doi.org/10.1016/S1464-1917(00)00072-6).
- [35] P.M. Mehta, S.N. Paul, N.H. Crisp, P.L. Sheridan, C. Siemes, G. March, S. Bruinsma, Satellite drag coefficient modeling for thermosphere science and mission operations, *Adv. Space Res.* (2022) <http://dx.doi.org/10.1016/j.asr.2022.05.064>.
- [36] N. Wallace, P. Jameson, C. Saunders, M. Fehring, C. Edwards, R. Floberghagen, The GOCE ion propulsion assembly – lessons learnt from the first 22 months of flight operations, in: 32nd International Electric Propulsion Conference, Wiesbaden, Germany, IEPC-2011-327, 2011.
- [37] V.G. Tirila, A. Demairé, C.N. Ryan, Review of alternative propellants in hall thrusters, 2023, <http://dx.doi.org/10.1016/j.actaastro.2023.07.047>.
- [38] P.A. Chambre, S.A. Schaaf, *Flow of Rarefied Gases*, Princeton University Press, 1961, <http://dx.doi.org/10.1515/9781400885800>.
- [39] SLATS/tsubame, 2012, <https://www.eoportal.org/satellite-missions/slats#overview>. (Accessed 06 July 2023).
- [40] L.A. Sinpetru, N.H. Crisp, D. Mostaza-Prieto, S. Livadiotti, P.C. Roberts, ADBSat: Methodology of a novel panel method tool for aerodynamic analysis of satellites, *Comput. Phys. Comm.* 275 (2022) 108326, <http://dx.doi.org/10.1016/j.cpc.2022.108326>.
- [41] GOMspace website, 2023, <https://gomspace.com/home.aspx>. (Accessed 06 July 2023).
- [42] FreeCAD website, 2023, <https://www.freecad.org/>. (Accessed 06 July 2023).
- [43] M.D. Pilinski, B.M. Argrow, S.E. Palo, Semiempirical model for satellite energy-accommodation coefficients, *J. Spacecr. Rockets* 47 (6) (2010) 951–956, <http://dx.doi.org/10.2514/1.49330>.
- [44] L.A. Sinpetru, N.H. Crisp, P.C. Roberts, V. Sullioti-Linner, V. Hanessian, G.H. Herdrich, F. Romano, D. Garcia-Almiñana, S. Rodríguez-Donaire, S. Seminari, ADBSat: Verification and validation of a novel panel method for quick aerodynamic analysis of satellites, *Comput. Phys. Comm.* 275 (2022) 108327, <http://dx.doi.org/10.1016/j.cpc.2022.108327>.